Table V—Calculated Values of A, B, α, and β Utilizing the Curve-Stripping Procedure for Acid Halide Catalysis

pH	Temperature	$[Cl^-]$, M	A, M	B, M	$\alpha \times 10^{-3}$, min^{-1}	$\beta \times 10^{-4}$, min^{-1}
1.10	37°	0.10	0.127	2.323	16.8	9.2
	37°	0.033	0.127	2.323	8.1	3.64
	47°	0.10	0.175	2.275	84.75	24.2
	47°	0.033	0.175	2.275	21.9	8.7
	47°	0.01	0.175	2.275	10.76	3.4
	57°	0.10	0.262	2.188	154.0	58.34
	57°	0.033	0.262	2.188	49.8	21.50
	57°	0.01	0.262	2.188	23.5	9.67
1.50	57°	0.10	0.237	2.213	65.3	27.6
	57°	0.033	0.237	2.213	27.9	13.0
	57°	0.01	0.237	2.213	16.6	5.76
	67°	0.10	0.322	2.128	130.0	50.7
	67°	0.033	0.322	2.128	60.7	31.7
	67°	0.01	0.322	2.128	23.7	14.7

ronment in the extra- and intracellular fluids can be a good justification for the alteration of anionic release and, therefore, activity.

REFERENCES

(1) B. Rosenberg, L. Van Camp, and T. Krigas, *Nature*, **205**, 698 (1965).

(2) B. Rosenberg, L. Van Camp, J. E. Trasko, and V. E. Mansour, *ibid.*, **222**, 385 (1969).

(3) J. A. Howle, G. R. Gale, and A. B. Smith, *Biochem. Pharmacol.*, **21**, 1465 (1972).

(4) A. B. Robins, *Chem.-Biol. Interact.*, **6**, 35 (1973).

(5) D. R. Williams, *Inorg. Chim. Acta Rev.*, **6**, 123 (1972).

(6) J. E. House, Jr., and M. J. Adams, *J. Inorg. Nucl. Chem.*, **32**, 345 (1970).

(7) R. Farrou and J. E. House, Jr., *ibid.*, **34**, 2219 (1972).

(8) L. I. Elding and L. Gustafson, *Inorg. Chim. Acta*, **5**, 643 (1971).

(9) L. I. Elding, *ibid.*, **6**, 647 (1972).

(10) *Ibid.*, **6**, 683 (1972).

(11) *Ibid.*, **7**, 581 (1973).

(12) D. Robb, N. M. De V. Steyn, and H. Kruger, *Inorg. Chim. Acta*, **3**, 383 (1969).

(13) A. J. Poe and D. H. Vaughan, *ibid.*, **1**, 255 (1967).

(14) R. G. Pearson and D. A. Johnson, *J. Am. Chem. Soc.*, **86**, 3983 (1964).

(15) J. S. Coe, J. R. Lyons, and M. D. Hussain, *J. Chem. Soc. A, Part I*, **1970**, 90.

(16) J. S. Coe, M. D. Hussain, and A. A. Malik, *Inorg. Chim. Acta*, **2**, 65 (1968).

(17) R. F. Coley and D. S. Martin, Jr., *ibid.*, **7**, 573 (1973).

(18) J. S. Coe and J. R. Lyons, *J. Chem. Soc. A, Part III*, **1969**, 2669.

(19) C. M. Davidson and R. F. Jameson, *Trans. Faraday Soc.*, **61**, 2462 (1965).

(20) H. A. Tayim, A. H. Malakian, and A. B. Bikhazi, *J. Pharm. Sci.*, **63**, 1469 (1974).

(21) C. E. Skinner and M. M. Jones, *J. Am. Chem. Soc.*, **91**, 1984 (1969).

ACKNOWLEDGMENTS AND ADDRESSES

Received November 24, 1975, from the *School of Pharmacy and the ‡Chemistry Department, American University of Beirut, Beirut, Lebanon.

Accepted for publication December 8, 1976.

Presented at the Basic Pharmaceutics Section, APhA Academy of Pharmaceutical Sciences, Atlanta meeting, November 1975.

Supported in part by a grant from the University Medical Research Fund, American University of Beirut.

ˣ To whom inquiries should be directed.

Microbiological Turbidimetric Methods: Linearization of Antibiotic and Vitamin Standard Curves

F. KAVANAGH

Abstract □ Procedures were devised to linearize the usually curved calibration lines for turbidimetric microbiological assays. Three new equations relating concentration of drug and turbidity are described; two are for antibiotic assays and one for vitamin assays. One equation is for antibiotic assays employing *Klebsiella pneumoniae* as the test organism. The accuracy of interpolation from the three equations was studied by means of appropriate mathematical models based on erythromycin, chlortetracycline (*K. pneumoniae*), and cyanocobalamin assays. The accuracy of the new expressions was significantly superior to those used previously, and they are of general applicability.

Keyphrases □ Microbiological turbidimetry—antibiotic and vitamin assays, procedures devised to linearize curved calibration lines □ Turbidimetry—microbiological antibiotic and vitamin assays, procedures devised to linearize curved calibration lines □ Antibiotics—microbiological turbidimetry assays, procedures devised to linearize curved calibration lines □ Vitamins—microbiological turbidimetry assays, procedures devised to linearize curved calibration lines

Nonlinear standard curves are much more common than straight lines in microbiological turbidimetric assays for growth-promoting substances and antibiotics. The nonlinear calibration line is particularly important in high accuracy assays because of the difficulty of obtaining sample potencies from it with negligible computational error. High accuracy assays are now possible not only from the automated system previously described (1) but also from manual assays. Therefore, the old practice of drawing a "best" straight line through the points of the standard line is no longer appropriate because the line, in reality, is curved. Approximating the slightly curved antibiotic lines by straight-line segments (2, 3) causes a small computational error.

Procedures for straightening both the antibiotic lines and the often more strongly curved vitamin lines are described in this report. Antibiotic lines will be considered separately from vitamin lines because they have different theoretical bases and the procedures have different principles.

Since an equation that truly fits a calibration line is not known, the line can only be approximated. The approximation can be fairly accurate when calibration points are close together. However, if the dose line can be linearized, fewer calibration points are needed to obtain the same accuracy of approximation. The aim of the present study

Table I—Model of *K. pneumoniae* Automated Antibiotic Assays

Sample Concentration[a]	Standards 1.6, 2, 2.4, 3.2, and 4 with Potencies Interpolated from Best Straight Line: *A versus* log *C*		Standards 1.6, 2.4, 3.2, and 4 with Potencies Interpolated from Point to Point: log $(A + M)$ *versus* C^2	
	0.1[b]	0.15	0.1	0.15
1.8	1.829	1.805	1.799	1.797
2.0	1.939	1.946	1.999	1.997
2.5	2.297	2.384	2.500	2.501
2.8	2.577	2.700	2.801	2.804
3.0	2.796	2.928	3.000	3.003
3.5	3.468	3.538	3.495	3.499
3.6	3.625	3.662	3.595	3.599

[a] Concentration in arbitrary units. [b] Sample volume.

was to achieve a linearization procedure so that interpolation errors are less than 0.25% of potency when the number of standards is five or less. The procedures given here increase the workload of the computer normally used to acquire and process the data by an insignificant amount. If maximum accuracy is needed only occasionally, calculations are practical with desk-top calculators or certain programmable pocket calculators.

Procedures for obtaining potencies with minimum computational errors are needed before naive statistical calculations are undertaken. Biases caused by inappropriate calculations should not become part of an answer or be involved in a validity test of the assays. Statistical procedures designed for both manual and automated assays will be considered in a subsequent publication.

EXPERIMENTAL

Data were obtained from semiautomated assays for cyanocobalamin, erythromycin, and chlortetracycline.

Test Organisms and Media—*Staphylococcus aureus* (ATCC 9144) was used in the erythromycin assay, *Klebsiella pneumoniae* (ATCC 10031) was used in the chlortetracycline assay, and *Lactobacillus leichmannii* (ATCC 7830) was used in the cyanocobalamin assay.

Commercial antibiotic assay broth No. 3 was used for all antibiotic assays. Commercial medium was used for the cyanocobalamin assay.

Assay Procedures—Procedures for erythromycin (4) and chlortetracycline were described previously (5). The cyanocobalamin method was a USP method adapted to the semiautomated system.

The design and operation of the semiautomated turbidimetric assay system were described recently (1–3, 6, 7). The automated diluter produces assay tubes containing about 0.10 or 0.15 ml of sample.

The chlortetracycline assay was essentially that for penicillin (8) modified to employ *K. pneumoniae* (5).

Calibration Lines for Antibiotics—The quality of an assay depends in part upon how well the calibration line describes reality. Ideally, potencies obtained from a dose line should not contain any error attributable to the form of the line. Such error increases bias and complicates conclusions from tests for invalidity. The many dose lines (9) used have different curvatures and, consequently, different errors caused by linear interpolation. The best practical form needs to be found to obtain potencies of test preparations and for validity testing.

The theoretical dose–response line (3) for an antibiotic that reduces the growth rate of the test organism is:

$$N_t = N_0 \exp[k_0 + f(v)k_m - k_aC]t \qquad \text{(Eq. 1)}$$

where N_t is the concentration of bacteria after an incubation period of t, N_0 is the concentration of bacteria in the assay tubes at the beginning of incubation, k_0 is the generation rate constant in the absence of antibiotic, C is the concentration of antibiotic with an inhibitory coefficient k_a, k_m represents the menstruum effect, and $f(v)$ is a function of the volume of sample added to the assay tube.

Equation 1 is used only as a guide to thought because usually N_0, k_0, $f(v)$, k_m, k_a, and t are unknown. In a particular assay, they are constant in all assay tubes; otherwise, the assay is invalid. Therefore, Eq. 1 can be written in an equivalent form as:

$$\log N = G + BC \qquad \text{(Eq. 2)}$$

where G and B are constant in an assay and dependent on details. Conversion of transmittance of the bacterial suspensions into corresponding values of N is by means of a calibration equation.

Since absorbance, A, is much more convenient to use than N in computing potencies in assays, it was used in Eq. 3 to give the absorbance analog of Eq. 2:

$$\log A = E + FC \qquad \text{(Eq. 3)}$$

Equation 3 was modified to straighten the line:

$$\log (A + M) = O + PC \qquad \text{(Eq. 4)}$$

The value and algebraic sign of M were chosen to make the line straight over the region of interest. For *K. pneumoniae* assays, Eq. 4 was modified by substituting C_2 for C:

$$\log (A + M) = R + SC^2 \qquad \text{(Eq. 5)}$$

The value of M in Eqs. 4 and 5 may be zero and the algebraic sign may be + or −. The sign is negative if the log A *versus* C line curves away from the C axis at the higher values of C and is positive if the line curves toward the C axis.

The constant M is introduced to compensate for two sources of curvature: the actual nonlinear relationship between log N and C and the nonlinear response of the photometer. To obtain the least computational error, assay responses should be corrected for photometer response before interpolating from Eqs. 4 and 5. The values of M in these equations are computed to minimize $(\text{error})^2$ for standard responses. Photometer correction is a function of the test organism, wavelength, and instrument (9).

A relationship favored by official bodies and statisticians is a plot of log dose *versus* some response of the photometer (10, 11). Both absorbance and transmittance are used as the response. The absorbance version is given as:

$$A = R + S \log C \qquad \text{(Eq. 6)}$$

and the transmittance version is:

$$T = U + V \log C \qquad \text{(Eq. 7)}$$

Testing the equations by means of a few actual assays was inappropriate because of differences caused by variations in operations. Statistical evaluation of many assays would reveal the preferred dose line. Instead, a mathematical procedure was employed using a model derived from an erythromycin assay.

Model 1 was constructed as follows. Measured absorbances of standards of an automated assay were converted into relative concentration, N, of bacteria by means of a calibration equation (9). These values of N were plotted according to Eq. 2. The lines were curved. Several trials showed that subtracting a constant number from N and plotting the resultant values against concentration gave essentially straight lines. A straight line was drawn through the points corresponding to concentrations 1 and 5, and the coefficients for the lines were calculated.

These equations were used to calculate values of N for each standard concentration and for each of the four "samples" with six-place accuracy. The photometer calibration line was used to find the absorbance corresponding to each N. Transmittances were calculated from the absorbances. These values of N, A, and T represent the values of C with error only in the sixth place, an error too small to be significant in testing forms of response lines.

Six equations were tested to find the one with the least computational

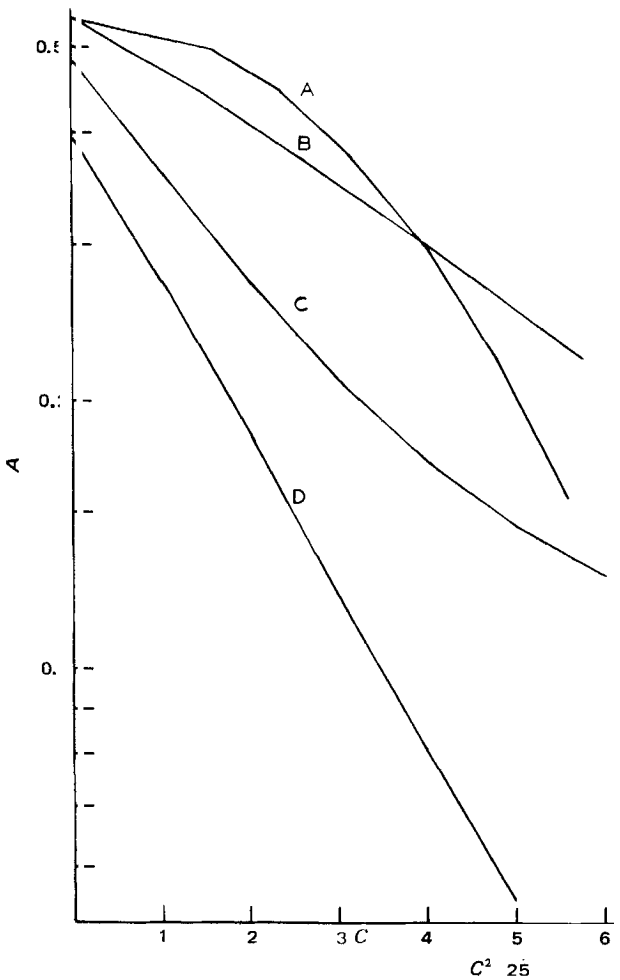

Figure 1—*Standard lines for Models 1 and 2. Key: A, Eq. 3 for Model 2; B, Eq. 5 for Model 2,* M = *0; C, Eq. 3 for Model 1; and D, Eq. 4 for Model 1,* M = *0.09. Responses are given as log* A *or log* (A − M) versus C *or* C^2.

error. Since testing the equations at all points is impossible, they were tested at concentrations midway between calibration points where error may be greatest. Appropriate values of A or T were substituted in them, and concentrations of "samples" were calculated by linear interpolation between bracketing standards or from the best straight lines through the standard responses. Goodness of fit of the several dose lines (Eqs. 2–7) to the true dose line was measured by taking the differences between the interpolated sample potencies and corresponding "potencies" of 1.5, 2.5, 3.5, and 4.5, squaring each difference, and summing to obtain the mean square error.

Because *K. pneumoniae* assays may be strongly curved, a separate model was designed. Model 2, based on a chlortetracycline assay, was constructed in exactly the same way as Model 1 except for substitution of C^2 for C in the equations. Graphs of Eq. 3 in both the C and C^2 versions are given in Fig. 1. Two slightly different designs were tested. One followed FDA practice (10) of spacing five standard concentrations on a logarithmic scale (Eq. 6). The multiplier was about 1.25. The actual concentrations were such that they could be prepared accurately by means of volumetric pipets and flasks. The best straight line through the five points, as required by the official method, was used to obtain "potencies" (Table I). The second set of calculations (Table I) followed a point-to-point version of Eq. 5 using only four standards.

The M in Eqs. 4 and 5 was computed for each three-point segment of the dose line and used for interpolating all potencies falling between end-points.

RESULTS

Since N, A, and T in the model computations were known with six-place accuracy, potencies computed for the samples should be free from error in the fifth place. Therefore, any differences between assigned and

Table II—Model 1 of Automated Antibiotic Assays with Potencies of Samples Interpolated from Three Equations Using Standards of 1, 2, 3, 4, and 5

	Best Straight Line: *A versus* log *C*		Point to Point			
			log *A versus C*		log (*A* + *m*) *versus C*	
Sample[a]	0.1[b]	0.15	0.1	0.15	0.1	0.15
1.5	1.442	1.497	1.509	1.525	1.497	1.498
2.5	2.481	2.707	2.518	2.542	2.503	2.503
3.5	3.573	3.704	3.526	3.558	3.499	3.499
4.5	4.538	4.352	4.534	4.569	4.500	4.501
10^4 (Error)^2	105	1064	22	105	0.2	0.2

[a] Concentration in arbitrary units. [b] Sample volume.

computed potencies represent a lack of fit of the calibration line to the reality of the model. The (error)^2 at the bottom of the table is a measure of the goodness of fit of the dose line to the points and is zero for a perfect fit.

Table II gives potencies computed for samples of Model 1. The results showed Eq. 4 to be better than Eq. 3 or 6. Equation 4 was applied to assays for bacitracin, chlortetracycline, cephaloridine, erythromycin, formaldehyde, furazolidone, hygromycin B, monensin, nitrofurantoin, penicillin G, phenol, tetracycline, thimerosal, and tylosin. The best straight line always gave larger errors than the point-to-point calculations from the same equation.

For Model 2, the results (Fig. 2 and Table I) indicate that the best straight line through the points of the standard (Eq. 6) is a very poor approximation of the true line. The deviations from the true values and the poor agreement between results at the two volumes of sample indicate considerable bias in the computations. Results in Table III show Eq. 5 to be superior to Eqs. 4, 6, and 7. Equation 5 has been applied to assays for chlortetracycline and streptomycin with *K. pneumoniae* as the test organism.

Computations using N in Eqs. 4 (Model 1) and 5 (Model 2) but not the others would have been without error. The (error)^2 shown in Table II for Eq. 4 (Model 1) and in Table III for Eq. 5 (Model 2) result from using uncorrected spectrophotometer responses. Absorbance corrected for the nonlinear response of the spectrophotometer is equivalent to N for calculation purposes. Therefore, to achieve minimum computational error, absorbances should be corrected for spectrophotometer response before substituting in Eq. 4 or 5. Values of M in Eqs. 4 and 5 are selected so that the resulting line is the best straight line through the points.

Computational procedures such as those discussed can be a source of additional errors when applied blindly. The first and last parts of the usual standard line are too flat to permit accurate assays and should be avoided regardless of the procedure. Generally, the usable part of a standard line lies between 20 and 80% of uninhibited growth (0 tube). This portion can be linearized by means of Eqs. 4 and 5. Each assay sys-

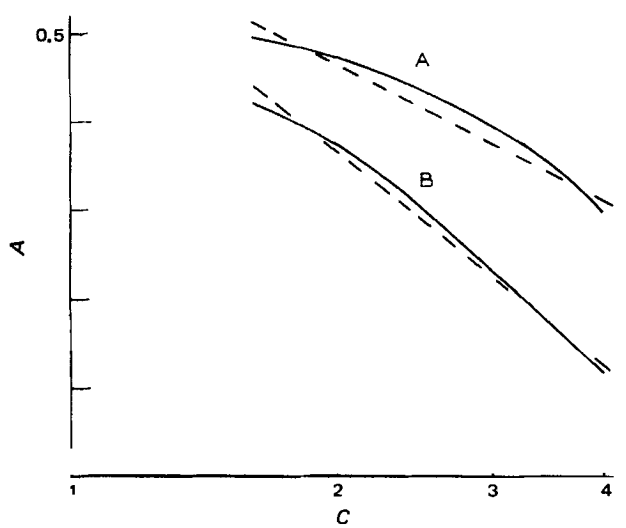

Figure 2—*Standard lines for Eq. 6 representing* K. pneumoniae *assays. Solid lines are smooth curves through the points. Dashed lines are the best straight lines through the five points. Lines A and B are for sample sizes 0.1 and 0.15 ml, respectively. FDA spacing of standards is followed. Responses are given as* A versus *log* C.

Table III—(Error)^2 for Model of *K. pneumoniae* Automated Antibiotic Assays [a]

	Standards 1.6, 2, 2.4, 3.2, 4						Standards 1.6, 2.4, 3.2, 4	
	Best Straight Line				Point to Point:		Using Point to Point:	
	A versus log *C*		*T versus* log *C*		log (*A* + 0.01) *versus C*		log (*A* + *M*) *versus* C^2	
Sample size	0.1	0.15	0.1	0.15	0.1	0.15	0.1	0.15
10^4 (Error)^2	1388	700	2444	1311	36	34	0.5	0.5

[a] Samples are same as those in Table II.

tem should be examined carefully to discover the portion of the standard line to use. The ratio of high to low concentrations may be twofold in some systems and as much as, but rarely more than, fivefold in others.

Calibration Lines for Vitamins—Nonlinear calibration lines are more common than straight lines in vitamin assays. Usually a smooth curve is drawn through the points plotted on graph paper, and sample potency is then interpolated from the curve. Such a procedure is suitable only for a low precision assay because of errors inherent in manual interpolation and in the inability to draw the true line through the points. The more nearly rectilinear is the line, the more accurately it can be drawn and interpolated from by hand or by computer. A nearly straight dose line and interpolation by computer must be used to achieve the potential in high accuracy assays. The assays can be done either manually or by automated systems (1).

Three quite different expressions are used to represent calibration lines in official turbidimetric methods: *T versus C* (11), *T versus* log *C* (12), and log *T versus* log *C* (12). The USP (12) specified that the line nearest to straight is to be used. Others use *A versus C* (13, 14) and *N versus C* (9), where *N* is the concentration of bacteria. The last expression is the dose–response line for growth-promoting substances. Substitution of *A* for *N* increases the curvature of the line because of the nonlinear response of photometers to suspensions (9). These calibration lines are plotted in Figs. 3–5 from the same set of responses for a cyanocobalamin assay.

Of the three forms used in official methods, *T versus* log *C* was the straightest. The line *N versus C*, the one with the theoretical basis, was straight over most of the range. The line *A versus C*, a first approximation to the theoretical one, was slightly curved because of the nonlinear spectrophotometer response.

The theoretical dose–response line for growth-promoting substances is for the limiting case and usually is simpler than reality. It applies when the only factor limiting growth is the one substance being assayed. In practice, a deficient medium, unfavorable growth conditions, and an incubation time too short to achieve limiting growth modify the relationship between *N* and *C* to increase curvature. In general, the *N versus C* dose–response line may be expected to be more strongly curved than the one in Fig. 3. The nonlinear response of the photometer to suspensions also causes curvature. Vitamin assays generally are grown to absorbances of 0.6 or more, and spectrophotometer corrections are relatively large at such absorbances. A large *A* has a proportionally greater correction than a small *A* (9). Therefore, the *A versus C* line curves more than the *N versus C* line.

A disadvantage to the dose–response line is the extra step caused by converting *T* to *N* by means of a calibration line (9). The calibration line for the conversion is a function of the optical properties of the test organism, wavelength of measurement, and geometry of the photometer (9). Since *A* is accurately obtainable from *T*, it is the preferred response metameter to be used in assaying.

Graphs of several assays for different vitamins employing different kinds of photometers had a lower straight portion. Curvature in the *A versus C* lines began at about *a* , 0.2 and then curved toward the *C* axis. The lines could be made essentially rectilinear by the transformation:

$$A' = A + B(A - D)^2 \qquad \text{(Eq. 8)}$$

where *D* is the value of *A* at the beginning of curvature. The calibration line for an assay then becomes:

$$C = E + FA' \qquad \text{(Eq. 9)}$$

However, *A* (not *A'*) is used in Eq. 9 when $A \leq D$.

Model of a Vitamin Assay—Data free from all error were needed to test Eq. 9 and to show the computation errors and biases caused by curved calibration lines. Since such data cannot be obtained from actual assays, they were derived from a model of a cyanocobalamin assay. The model, based on the theoretical dose–response line for growth-promoting substances, is:

$$C = G + HN \qquad \text{(Eq. 10)}$$

where *C* is the concentration of drug, *N* is the concentration of test organism, and *G* and *H* are constants. The line used in constructing this model curves at $N \geq 20$ ($C = 2$) in such a manner that it may be linearized by substituting:

$$N' = N + 0.012(N - 20)^2 \qquad \text{(Eq. 11)}$$

for *N* in Eq. 10 for values of $N > 20$.

A calibration line relating *N* and *A* for a *L. leichmannii* suspension measured at 650 nm is used to obtain *A* from *N*. Then *T* is calculated from *A*. The concentrations, *C*, are assigned values ranging from 0 to 10. The even digits are considered to be standards, and the odd digits are the samples. Values of *A* and *A'* are given in Table IV. The quality of the linearization is tested by comparing *C* computed from *A'* and the true value. Responses as *N*, *A*, and *A'* are given in Fig. 6.

The coefficients *B*, *D*, *E*, and *F* must be found before Eqs. 8 and 9 can be applied. Three responses, A_0, A_i, and A_j, at 0, C_i, and C_j are required; 0, A_0, C_i, and A_i are substituted in Eq. 9, and *E* and *F* are computed. Then A_j is computed for C_j from Eq. 9, and A_j, A_j', and $A_i = D$ are substituted in Eq. 8 to obtain *B*. Then the values of *A* corresponding to measured *A* for $A > D$ are computed from Eq. 8. The C_i is the standard nearest to the upper end of the straight portion of the *C versus A* line. This calculation causes the three points 0, C_i, and C_j to fall on a straight line according to Eq. 9; C_j should be near to the upper limit of the standards.

In the general case, the response line cannot be fitted by an equation

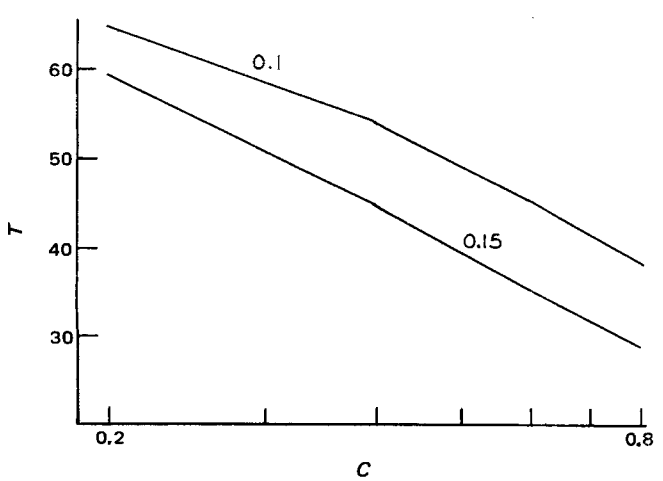

Figure 3—*Responses for a cyanocobalamin assay. Concentration of vitamin is nanograms per milliliter for sample tubes of the automated system. Responses are given as* T versus *log* C.

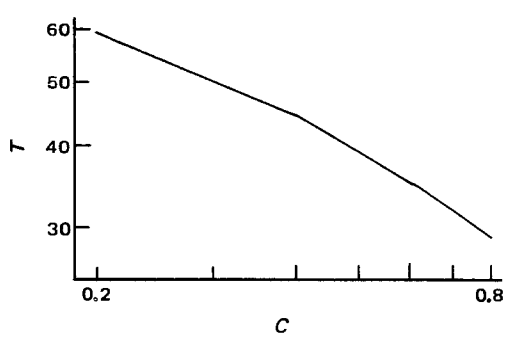

Figure 4—*Responses for a cyanocobalamin assay (same data as in Fig. 3). Responses are given as log* T versus *log* C.

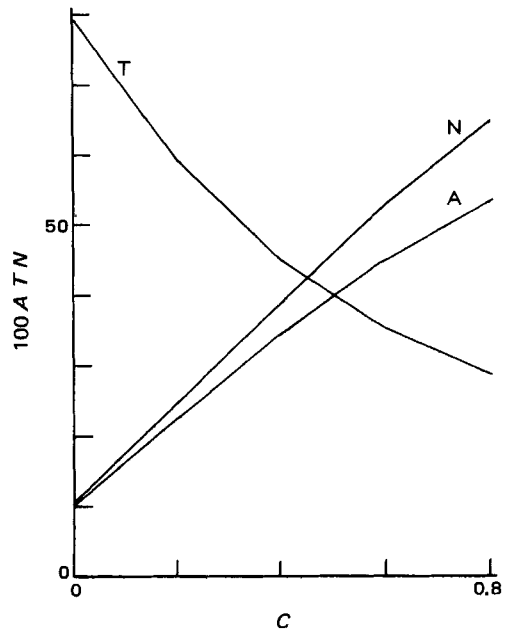

Figure 5—*Responses for cyanocobalamin assay (same data as in Fig. 3). Responses are given as* T versus C, A versus C, *and* N versus C, *where* T *is the percent transmittance,* A *is the absorbance, and* N *is the relative concentration of bacteria.*

as could the lines in Fig. 6, and potency is obtained by interpolation from a point-to-point line bracketing the sample.

The AOAC (11) procedure for vitamins does not indicate the kind of line to be drawn through the points of the standard line of the form *T versus C*. The USP procedure (12) provides the option of drawing either a straight line or a smooth curve through the plotted points of responses of the standards. The assumption was made that a smooth curve was drawn through the points. For interpolation purposes, the smooth curve was assumed to be quadratic in concentration. An equation was fitted to three standards such as 2, 4, and 6, and potency for the 3 and 5 samples was computed from it. Then the equation was fitted to standards 4, 6, 8, *etc.* This approach is a point-to-point procedure applied to a curved line.

Test of Several Calibration Lines—The values of *A* in Table IV after conversion into *T* were used to test dose lines of the forms *A versus C*, *A′ versus C*, *A versus* log *C*, *T versus* log *C*, and *T versus C* for computational error of interpolated potencies (Table V).

The linear *A versus C* relationship was worst followed by the curve *T versus C*. The others would be acceptable for most work at higher concentrations. The *A′ versus C* relationship was the best of the straight lines over the entire concentration range. For most of the range, computational errors were insignificant.

The parabola was no better than the procedure for linearization (Eq. 9) when *A′* was a quadratic function of *C*. However, *A* as a quadratic function of log *C* gave nearly error-free potencies for the samples when the equation was fitted to three contiguous points of the standard line. The quadratic equation was restricted to the curved part of the *A versus C* line. Fitting the equation to more than three standard points of the model increased the interpolation error.

Table IV—Responses in Model Vitamin Assays

C	*A*	*A′*
	Standards	
0	0	0
1	0.0925	0.0925
2	0.1850	0.1850
4	0.3255	0.3731
6	0.4255	0.5649
8	0.5042	0.7498
10	0.5692	0.9251
	Samples	
2	0.1850	0.1850
3	0.2626	0.2771
5	0.3789	0.4695
7	0.4669	0.6584
9	0.5381	0.8387

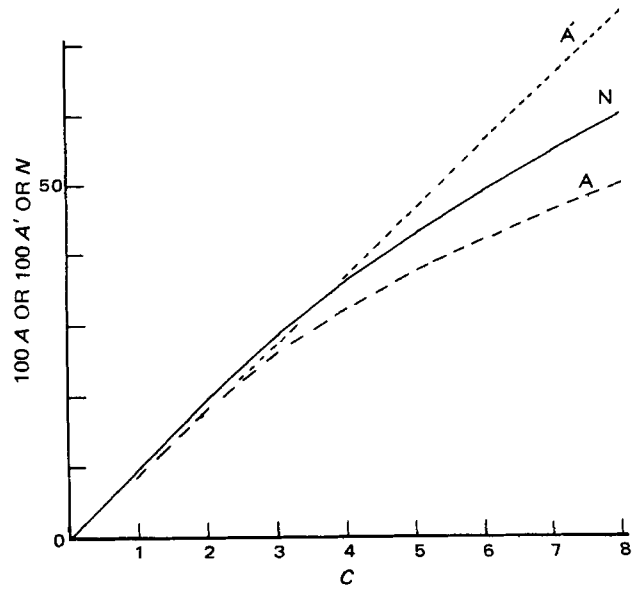

Figure 6—*The* A, N, *and* A′ *responses of the model of a vitamin assay.*

The procedure for straightening calibration lines of growth-promoting substances was applied to lines obtained in turbidimetric assays for thiamine (15), folic acid (16), pyridoxine (17), and cyanocobalamin (18) and to a titrimetric assay for niacin (19). The pyridoxine assay employing *Saccharomyces carlsbergensis* was so strongly curved that the high end correction (Eq. 8) was equal to the observed absorbance. Correction was much smaller for the other assays. The *A versus C* and *A′ versus C* lines for folic acid and pyridoxine standards are shown in Fig. 7.

Graphs of *A versus C* should form a smooth curve. Few graphs of published data were smooth, a not unexpected finding considering that the work was done before highly accurate assays were possible. An occasional rather large error was found such as, for example, a misidentified sample.

Selection of an interpolation formula to be used in an assay depends upon the quality of the assay, the curvature of the standard line, the accuracy needed, and computational facilities. The linear point-to-point versions of *A versus C*, *A′ versus C*, and *T versus* log *C* all are useful. The one giving the straightest line over the part of the standard line to be used in the assay should be selected. A parabola, *A versus* log *C*, fitted to three points may be better than a point-to-point straight line when sample responses fall within the span of three points on the standard line and calculations are done with a programmable calculator. The *N versus C* line is used to evaluate assay design and operations (9).

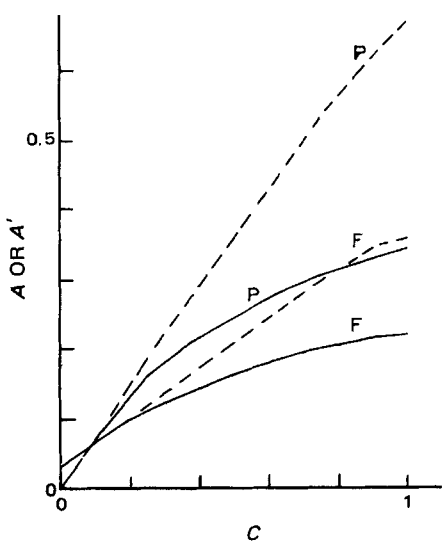

Figure 7—*The* A *and* A′ *lines for folic acid (16) and pyridoxine (17) assays. Solid lines are for* A versus C, *and dashed lines are for* A′ versus C. *The concentration scale is in arbitrary units.*

Table V—Point-to-Point Interpolations from Five Relationships between C and a Response Function for the Vitamin Model

Known C	Linear				Quadratic in C					
	A versus C		A' versus C		A versus log C		T versus C		T versus log C	
	C	Error, %	C	Error, %	C	Error, %	C	Error, %	C	Error, %
3	3.092	3.1	2.991	0.0	3.001	0.0	3.057	1.9	2.986	−0.5
5	5.063	1.2	5.006	0.1	5.000	0.0	4.929	−1.4	5.011	0.2
7	7.050	0.7	7.012	0.2	7.001	0.0	6.963	−0.5	7.005	0.1
9	9.042	0.5	9.015	0.2	9.001	0.0	8.796	−0.3	9.002	0.0

Graphical procedures are adequate when the assay is not of the highest quality or turbidity is measured with low precision and accuracy (±0.5% T). Computational procedures are appropriate for high quality automated assays.

SUMMARY

Common calibration lines for turbidimetric assays are more likely to be curved than straight. Fitting a best straight line to the points or even a point-to-point line causes errors in interpolated potencies. The closer the calibration line is to a straight line, the smaller will be the errors of interpolation.

Three new expressions, two for antibiotic assays and one for vitamin assays, that give straighter lines than those used previously were tested by means of three models based on real assays. The new expressions could be approximated much better by straight-line segments than could the older ones. The relationships used in official methods gave the largest computational errors. One new antibiotic equation was designed for assays employing *K. pneumoniae* as the test organism.

REFERENCES

(1) N. R. Kuzel and F. W. Kavanagh, *J. Pharm. Sci.*, **60**, 767 (1971).

(2) F. Kavanagh, *ibid.*, **60**, 1858 (1971).

(3) *Ibid.*, **64**, 844 (1975).

(4) F. Kavanagh, "Analytical Microbiology," vol. 2, Academic, New York, N.Y., 1972.

(5) H. S. Ragheb and A. M. Cummings, *J. Assoc. Offic. Anal. Chem.*, **57**, 527 (1974).

(6) N. R. Kuzel and F. W. Kavanagh, *J. Pharm. Sci.*, **60**, 764 (1971).

(7) F. W. Kavanagh, *ibid.*, **63**, 1463 (1974).

(8) F. Kavanagh and L. J. Dennin, in "Analytical Microbiology," F. Kavanagh, Ed., Academic, New York, N.Y., 1963, chap. 6.10.

(9) F. Kavanagh, "Analytical Microbiology," vol. 2, Academic, New York, N.Y., 1972, chap. 3.

(10) Code of Federal Regulations, Title 21, Part 436.106, 1974.

(11) "Official Methods of Analysis," 12th ed., Association of Official Analytical Chemists, Washington, D.C., 1975, 43.103.

(12) "The United States Pharmacopeia," 19th rev., Mack Publishing Co., Easton, Pa., 1975.

(13) L. Millbank, R. E. Davis, M. Rawlins, and A. H. Waters, *J. Clin. Pathol.*, **23**, 54 (1970).

(14) R. E. Davis, J. Moulton, and A. Kelly, *ibid.*, **26**, 494 (1973).

(15) E. Hoff-Jorgensen and B. Hansen, *Acta Chem. Scand.*, **9**, 562 (1955).

(16) A. H. Waters and D. L. Mollin, *J. Clin. Pathol.*, **14**, 335 (1961).

(17) W. Hewitt, "Microbiological Assay," Academic, New York, N.Y., 1977, Table 3.1.

(18) C. I. Bliss, *Bacteriol. Rev.*, **20**, 243 (1956).

(19) C. I. Bliss and C. White, in "The Vitamins," vol. VI, P. Gorgy and W. N. Pearson, Eds., Academic, New York, N.Y., 1967, p. 27.

ACKNOWLEDGMENTS AND ADDRESSES

Received October 18, 1976, from *231 Blue Ridge Road, Indianapolis, IN 46208.*

Accepted for publication January 6, 1977.

Skin as an Active Metabolizing Barrier I: Theoretical Analysis of Topical Bioavailability

H. Y. ANDO *, N. F. H. HO, and W. I. HIGUCHI ˣ

Abstract □ A model and explicit equations were developed to be used in the experimental design and data evaluation of situations where simultaneous metabolism and transport of drugs occur in the skin. By treating the skin as a two-ply laminate composed of the stratum corneum and the viable epidermis, which contains most of the catabolic enzymes that might render a drug inactive by metabolism, equations were developed permitting the *in vitro* assessment of factors that may affect topical bioavailability *in vivo*. Two situations were investigated. In the first, the drug was placed on the dermis side of the diffusion cell and did not penetrate the stratum corneum. In the second, the drug, placed on the epidermis side, penetrated the stratum corneum and then passed through the metabolizing epidermis. Expressions for determining the metabolic rate constant from experimental data along with concentration profiles and flux expressions are given both for the drug and its metabolite.

Keyphrases □ Bioavailability, topical—model and equations developed permitting *in vitro* assessment, assuming simultaneous metabolism and drug transport in skin □ Topical bioavailability—model and equations developed permitting *in vitro* assessment, assuming simultaneous metabolism and drug transport in skin □ Metabolism, drug—simultaneous with transport in skin, model and equations developed permitting *in vitro* assessment of bioavailability □ Transport, drug—simultaneous with metabolism in skin, model and equations developed permitting *in vitro* assessment of bioavailability

In the past, the major barrier to the delivery of a topical dosage form to the site of drug action has been considered to be the stratum corneum. The concept of the epidermis as a viable, metabolizing membrane, which can provide a metabolic barrier for drug action, has long been overshadowed by the emphasis on the passive permeability properties of the most superficial skin layer. Topical bioavailability should account for not only skin permeation but also cutaneous drug metabolism.

Studies concerning the passive permeability properties of the skin as a two-ply laminate (stratum corneum and viable epidermis) showed that drugs may enter the epidermis by breaching the stratum corneum and/or by passing through skin follicles, which may be considered